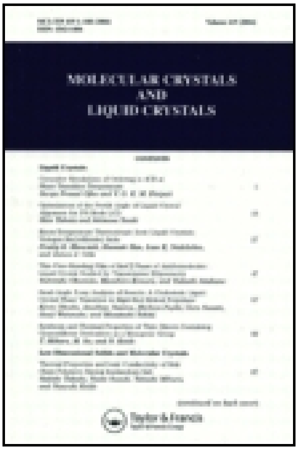

Molecular Crystals and Liquid Crystals

Publication details, including instructions for authors and subscription information:
http://www.tandfonline.com/loi/gmcl16

Lattice Models for Thermotropic Liquid Crystals

Martha A. Cotter [a] [b] [c]

[a] School of Chemisty, Rutgers University, New Brunswick, New Jersey, 08903

[b] Alfredd P. Sloan Foundation Research Fellow.

[c] Presently on leave at Bell Laboratories, Murray Hill, New Jersey, 07974

Version of record first published: 21 Mar 2007.

To cite this article: Martha A. Cotter (1976): Lattice Models for Thermotropic Liquid Crystals, Molecular Crystals and Liquid Crystals, 35:1-2, 33-70

To link to this article: http://dx.doi.org/10.1080/15421407608084310

Mol. Cryst. Liq. Cryst., 1976, Vol. 35, pp. 33–70
© Gordon and Breach Science Publishers, Ltd. 1976
Printed in Holland

Lattice Models for Thermotropic Liquid Crystals

MARTHA A. COTTER†‡
School of Chemistry, Rutgers University, New Brunswick, New Jersey, 08903

(*Received October 20, 1975*)

The utility of the DiMarzio–Alben lattice model for investigating thermotropic liquid crystals is evaluated, using a system of straight, inflexible rods with hard cores and nearest neighbor attractions on a simple cubic lattice. In the most general case, treated in the Bragg–Williams approximation, the rods, of length-to-breadth ratio x, are divided into a core portion of c segments and two "tail" portions of $(x - c)/2$ segments each and there are seven different segmental attractive energies: w_{cc}, w_{ct}, w_{tt}, w_{ee}, $w_{cc'}$, $w_{ct'}$, $w_{tt'}$, where c and t denote core and tail segments, respectively, unprimed and primed energies are for interactions between parallel and perpendicular rods, respectively, and w_{ee} is for the end-to-end interaction between the last segments of two parallel rods. In addition, a special case of the model is also treated in the quasi-chemical or Bethe approximation and the Bragg–Williams approach is extended to simple mixtures of hard rods of two different lengths with solvent–solvent, solvent–solute, and solute–solute attractions. By comparing the model predictions with experimental results, it is concluded that: (1) the lattice approach (or, for that matter, any molecular field treatment of a system of inflexible rods with hard cores and intermolecular attractions) does not appear to be useful for considering homologous series of pure nematogenic substances; however, it does seem to be of use for studying solute induced nematic → isotropic transitions in nematic solutions; (2) The quasichemical approach does not produce significantly better agreement with experiment than does the Bragg–Williams approach; (3) The model provides a qualitatively decent account of certain aspects of the smectic A → nematic phase transition, suggesting that more sophisticated lattice and/or cell models may be of use in treating both smectic A and more ordered smectic mesophases.

I INTRODUCTION

Liquid crystalline or mesomorphic systems are highly complex. Even on the phenomenological level, understanding of their behavior is incomplete. On the molecular level, it has been recognized for some time[1] that the magnitude and temperature dependence of the long range orientational order in

---

† Alfred P. Sloan Foundation Research Fellow.

‡ Presently on leave at Bell Laboratories, Murray Hill, New Jersey 07974.

nematic mesophases can be predicted semi-quantitatively using a mean field one-body attractive potential of the form

$$V_i = A(\rho)[\tfrac{3}{2}\cos^2\theta_i - \tfrac{1}{2}], \tag{1}$$

where θ_i is the angle between the long axis of a molecule and the preferred direction and ρ is the number density. Otherwise, however, very little is known concerning the position and orientation dependence of the intermolecular pair potential in nematic, smectic, or cholesteric systems. This ignorance, together with the size and complexity of the component molecules and the horrendous many-body aspects of the problem, make a reasonably realistic statistical mechanical treatment of liquid crystals clearly impossible at present. It is possible, however, to treat certain highly idealized liquid crystal-like models and, in so doing, to investigate the way in which selected molecular characteristics contribute to the stability and properties of various mesophases. To date, most such theoretical work has utilized either

1) mean field calculations
2) hard rod models.

The two approaches are in fact complementary: the mean field calculations have emphasized the role of anisotropic intermolecular attractions in determining mesomorphic behavior, whereas the hard rod calculations have emphasized the role of anisotropic intermolecular repulsions (i.e., packing effects). In real systems at liquid densities one would expect both factors to be quite important; and this supposition is supported by the work of Deloche, Cabane, and Jerome[2] and of McColl and Shih.[3]

The original mean field theory of nematic mesophases was that of Maier and Saupe,[1] who considered only dipolar dispersion forces between molecules and used a potential of the form (1). The theory has been extended, by the inclusion of other contributions to the intermolecular pair potential, by Humphries, James and Luckhurst[4] and by Chandrasekhar and Madhusudana[5] among others. More recently, the molecular field approach has been applied to smectic mesophases[6–9] and to a system of molecules with rigid central portions and semi-flexible end-chains.[10] The latter calculations, by Marčelja, utilized Flory's rotational isomeric model[11] to enumerate end-chain conformations and satisfactorily explained for the first time the odd–even effect in nematic → isotropic transition temperatures along homologous series of nematogens.

In hard rod model systems, the molecules are assumed to have hard (i.e., impenetrable) rodlike cores, with or without superimposed intermolecular attractions. A number of statistical mechanical techniques have been applied to fluids of inflexible rods, including cluster expansions,[12–13] scaled particle theory,[14–17] and lattice statistics.[18–21] In addition, hard particles with rigid cores and semi-flexible "tails" have been considered, using lattice models.[22–23] Although semi-quantitative agreement with experiment of the sort obtained from mean field calculations (frequently with the aid of one or more adjustable parameters) has not been obtained using hard rods, the latter approach has the advantages that the intermolecular potential is precisely defined and the model results can more readily be related to molecular structure and geometry.

Of the various approaches to hard rod fluids, the crudest are undoubtedly those utilizing lattice models, since these require restricting the molecular centers to a discrete ordered set of lattice sites and restricting the molecular long axes to a small number of discrete orientations, neither of which is very realistic for an anisotropic fluid. (The consequences of these constraints will be discussed later.) However, despite these obvious drawbacks, lattice models are appealing in certain respects. They are more tractable and therefore more widely applicable than (translational and rotational) continuum models. Unlike more physically appealing approaches such as scaled particle theory, lattice treatments can be extended readily to systems with quite complex attractive interactions as well as hard core repulsions. The remainder of this paper is devoted to a determination of the usefulness of lattice models for studying thermotropic liquid crystals. A lattice model, applicable to smectic A, nematic, and isotropic liquid phases is presented in Section II and solved in the Bragg–Williams or random mixing approximation in Section III. In Section IV, a special case of the general model is treated in the quasi-chemical or Bethe–Guggenheim approximation. Numerical results are presented and evaluated in Section V and certain conclusions concerning the utility of lattice models are drawn in Section VI.

II THE LATTICE MODEL

The model system consists of N rodlike molecules (rods) of length-to-breadth ratio x on a simple cubic lattice of M sites or cells of volume v_0. Each rod, of volume xv_0 has an inflexible core portion of c segments and two inflexible "tails" of $(x - c)/2$ segments, and occupies x adjacent nearest neighbor sites. There are, therefore, only three allowed mutually perpendicular molecular orientations, which shall be denoted by 1, 2, and 3, respectively. The rods are hard in that two rod segments cannot occupy the same lattice site; in addition, directly adjacent segments on neighboring rods attract one another with one of several segmental interaction energies; namely, w_{cc}, w_{ct}, w_{tt}, $w_{cc'}$, $w_{ct'}$, $w_{tt'}$, and w_{ee}, where c and t indicate core and tail segments respectively; unprimed and primed energies, respectively, are for interactions between parallel and perpendicular rods, and w_{ee} is for the end-to-end interaction of the last segments of two parallel rods. The number of rods pointing in each of the three allowed directions will be denoted by N_1, N_2, and N_3, respectively. In treating the nematic/isotropic liquid, it will be assumed that no translational

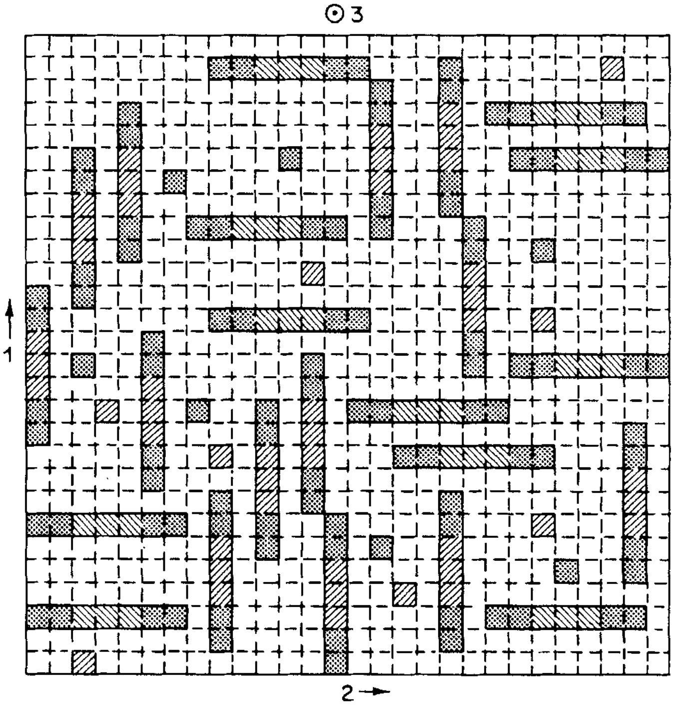

FIGURE 1 A visualization of part of the model system, seen in cross-section, at moderate density. The dashed lines represent the underlying lattice; filled-in sites represent rod segments. ▨ are core segments, while ▒ are tail segments. For the rods shown, $x = 7$ and $c = 3$.

order is present and $\{N_1, N_2, N_3\}$ will be determined by minimizing the Helmholtz free energy at constant N and M. In the lattice analog of the smectic A phase, on the other hand, it will be assumed that the rods are arranged in layers with all rod axes pointing in the same direction, normal to the plane of the layers. Part of the model system is pictured in Figure 1; the various types of segmental interactions are illustrated in Figure 2.

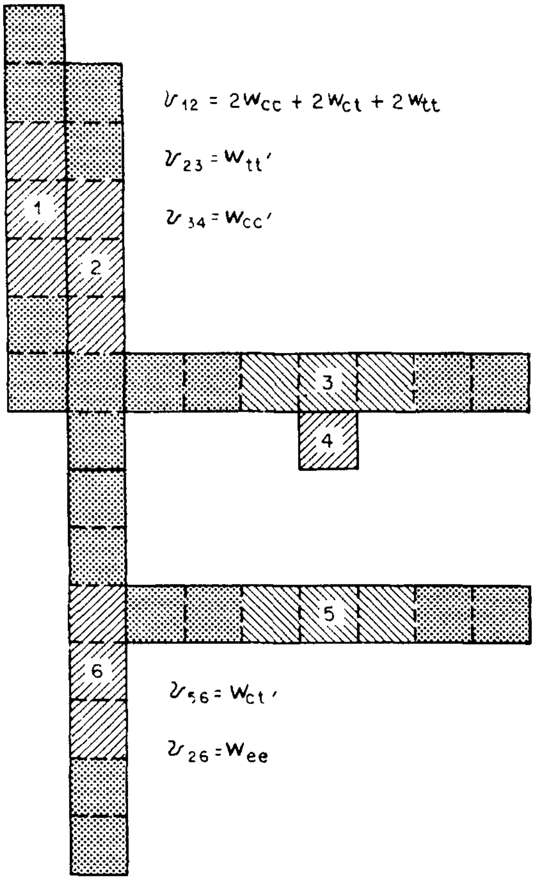

FIGURE 2 A cluster of six rods, illustrating the meaning of the various segmental attractive energies. v_{ij} is the total potential energy of interaction between rods i and j.

III BRAGG–WILLIAMS TREATMENT

A Nematic and Isotropic Phases

In the absence of long range translational order, the exact configurational partition function for the model system is given formally by

$$Q_c(N, M, T) = \sum_{N_1, N_2, N_3} \sum_{j_c} \exp(-E_{j_c}(N_1, N_2, N_3, M)/kT)$$

where k is Boltzmann's constant, T is absolute temperature, j_c represents the jth allowed configurational state (with energy E_{j_c}) for a given N_1, N_2, and N_3, and

$$\sum_{i=i}^{3} N_i = N \tag{3}$$

for each term in the multiple sum. In the Bragg–Williams or random mixing approximation, this exact expression is replaced by

$$Q_c(N, M, T) = \sum_{N_1, N_2, N_3} \Omega(N_1, N_2, N_3, M)\exp(-\bar{E}_c(N_1, N_2, N_3, M)kT) \tag{4}$$

where $\Omega(N_1, N_2, N_3, M)$ is the total number of allowed configurations for a particular N_1, N_2, and N_3; i.e., the total number of ways to arrange N_1 hard rods in direction 1, N_2 hard rods in direction 2, and N_3 hard rods in direction 3 on a lattice of M sites, and $\bar{E}_c(N_1, N_2, N_3, M)$ is the average configurational energy obtained by weighting all allowed configurations equally. In the limit $N \to \infty$, $M \to \infty$, N/M finite, the sum in Eq. (4) can be replaced by its maximum term, giving

$$Q_c(N, M, T) = \Omega(N_1^*, N_2^*, N_3^*, M)\exp(-\bar{E}_c(N_1^*, N_2^*, N_3^*, M)kT) \tag{5}$$

where $\{N_1^*, N_2^*, N_3^*\}$ is that set which maximizes $\Omega e^{-\bar{E}_c/kT}$. Since only nearest neighbor interactions are included in the model,

$$\bar{E}_c = \bar{N}_{cc}w_{cc} + \bar{N}_{ct}w_{ct} + \bar{N}_{tt}w_{tt} + \bar{N}_{cc'}w_{cc'} + \bar{N}_{ct'}w_{ct'} + \bar{N}_{tt'}w_{tt'} + \bar{N}_{ee}w_{ee} \tag{6}$$

where $\bar{N}_{cc}$, $\bar{N}_{ct}$, etc. are the average numbers of pairs of adjacent segments of the various types and, of course, depend on N_1^*, N_2^*, N_3^*, and M. Both Ω and $\bar{E}_c$ can be determined using the approximate configuration counting technique of DiMarzio,[19] which is based on a general procedure devised by Fory.[24]

In the Flory–DiMarzio approach, Ω is determined by placing the rods on the lattice one-by-one, i.e.,

$$\Omega(N_1, N_2, N_3, M) = \frac{\prod_{n=0}^{N-1} v_{n+1}^{(k)}}{\prod_{i=1}^{3} N_i!} \tag{7}$$

where $v_{n+1}^{(k)}$ is the number of ways to place the $(n + 1)$ st rod, with orientation k on the lattice.[25] But, to a high degree of accuracy,

$$v_{n+1}^{(k)} = (M - xn)(p_n^{(k)})^{(x-1)} \tag{8}$$

where $p_n^{(k)}$ is the probability that with the n rods present the adjacent site in direction k to the end of a rod being "constructed" in direction k is empty (i.e., $\nu^{(k)}_{n+1}$ is equal to the number of ways to add the first segment of rod $n + 1$ multiplied by the probability that the other $x - 1$ segments can be added successfully). Neglecting all local deviations from the mean density and orientational distribution of the rods already present,

$$p^{(k)}_n = \frac{M - xn}{M - xn + n_k + x\sum_{j\neq k} n_j} = \frac{M - xn}{M - (x - 1)n_k} \tag{9}$$

(n_i = number of rods present in orientation i), since the adjacent site in direction k *could* be empty or be occupied by the end of a rod in direction k or be occupied by any one of the x segments of any perpendicular rod. Inserting (8) and (9) into (7) and evaluating the product,[26] one obtains DiMarzio's expression for Ω, namely,

$$\Omega(N_1, N_2, N_3, M) = \frac{\prod_{i=1}^{3} [M - (x - 1)N_i]!}{(\prod_{i=1}^{3} N_i!)(M!)^2} \tag{10}$$

$\bar{E}_c(N_1, N_2, N_3, M)$ can be evaluated using the same sort of reasoning. Let $p^{(k)}_{\sigma i;\tau j}$ equal the probability that the adjacent segment in direction k to a segment of type $\sigma(\sigma = c, t)$ on a rod in direction i is occupied by a segment of type τ on a rod in direction j. Then, for example

$$\begin{aligned}\bar{N}_{ct} &= \sum_{i=1}^{3} 2cN_i \sum_{k\neq i} p^{(k)}_{ci;ti} = \sum_{i=1}^{3} 2cN_i \sum_{k\neq i} \frac{(x - c)N_i}{M - (x - 1)N_k}\\ &= 2c(x - c)\sum_{i=1}^{3} N_i^2 \sum_{k\neq i}\left[\frac{1}{M - (x - 1)N_k}\right];\end{aligned} \tag{11}$$

$$\begin{aligned}\bar{N}_{ct'} &= \sum_{i\neq j} 2cN_i[p^{(j)}_{ci,tj} + p^{(k)}_{ci,tj}]\\ &= \sum_{i\neq j} 2cN_i\left[\frac{N_j}{M - (x - 1)N_j} + \frac{(x - c)N_j}{M - (x - 1)N_k}\right]\\ &= 2c\sum_{i\neq j} N_iN_j\left[\frac{1}{M - (x - 1)N_j} + \frac{(x - c)}{M - (x - 1)N_k}\right] \qquad (k \neq i \text{ or } j).\end{aligned} \tag{12}$$

$\bar{N}_{cc}$, $\bar{N}_{cc'}$, $\bar{N}_{tt}$, $\bar{N}_{tt'}$, and $\bar{N}_{ee}$ can be derived in the same manner.

At this point it is convenient to single out direction 1 by means of some device such as an infinitesimal applied field and to assume that the equilibrium orientational distribution (N_1, N_2, N_3) is symmetric about this preferred direction. (This assumption is certainly true in uniaxial phases.) Then, inserting the expressions for $\bar{N}_{cc}$, $\bar{N}_{cc'}$, etc. into (6), introducing the reduced variables

$$\begin{aligned} s &= \frac{N_2^*}{N} = \frac{N_3^*}{N} \\ f &= \frac{xN}{M}, \end{aligned} \tag{13}$$

and simplifying, one obtains

$$\frac{\bar{E}_c}{N}(N_1^*, N_2^*, N_3^*, M) = \frac{2f}{x}\left\{\frac{Q_3}{Q_1} + \frac{Q_4}{Q_2}\right\} \tag{14}$$

where
$$\begin{aligned} Q_1 &= 1 - \left(1 - \frac{1}{x}\right)(1 - 2s)f, \\ Q_2 &= 1 - \left(1 - \frac{1}{x}\right)sf, \\ Q_3 &= (1 + \delta)W_2 s^2 + W_1 s(1 - 2s) + \frac{w_{ee}}{2}(1 - 2s)^2, \\ Q_4 &= (\delta W_2 + W_1 + w_{ee})s^2 + (2W_2 + W_1)s(1 - 2s) + \delta W_2(1 - 2s)^2, \end{aligned}$$

$$\delta = \frac{w_{cc}}{w_{cc'}} = \frac{w_{ct}}{w_{ct'}} = \frac{w_{tt}}{w_{tt'}}, \tag{15}$$

$$\begin{aligned} W_1 &= 2cw_{ct'} + 2(x - c)w_{tt'}, \\ W_2 &= c^2 w_{cc'} + 2c(x - c)w_{ct'} + (x - c)^2 w_{tt'} \end{aligned}$$

and we have assumed that all unprimed segmental interaction energies differ from their primed counterparts by the same multiplicative "anisotropy factor" δ. We now can evaluate Q_c and from it obtain the configurational part of any equilibrium thermodynamic quantity. In particular,

$$\begin{aligned} \frac{A_c}{NkT} = -\frac{\ln Q_c}{N} = \frac{x}{f}\{&(1 - f)\ln(1 - f) - Q_1 \ln Q_1 - 2Q_2 \ln Q_2\} \\ &+ (1 - 2s)\ln(1 - 2s) + 2s \ln s + \ln\left(\frac{f}{x}\right) \\ &+ \frac{2f}{xkT}\left[\frac{Q_3}{Q_1} + \frac{Q_3}{Q_2}\right], \end{aligned} \tag{16}$$

$$\begin{aligned} \frac{S_c}{Nk} = \frac{x}{f}\{Q_1 \ln Q_1 + 2Q_2 \ln Q_2 - (1 - f)\ln(1 - f)\} - \ln\left(\frac{f}{x}\right) \\ -(1 - 2s)\ln(1 - 2s) - 2s \ln s, \end{aligned} \tag{17}$$

$$\Phi(f, s) = \frac{Pv_0}{kT} = -\left[\frac{\partial}{\partial M}\left(\frac{A_c}{kT}\right)\right]_{N,T} = \ln Q_1 + 2\ln Q_2 - \ln(1-f) + \frac{2f^2}{x^2kT}\left[\frac{Q_3}{Q_1^2} + \frac{Q_4}{Q_2^2}\right], \tag{18}$$

$$\frac{\mu_c}{kT}(f, s) = \left[\frac{\partial}{\partial N}\left(\frac{A_c}{kT}\right)\right]_{M,T} = 2s\ln s + (1-2s)\ln(1-2s) + (x-1)[\ln Q_1 + \ln Q_2] - x\ln(1-f) + \ln\left(\frac{f}{x}\right) + \frac{2f}{xkT}\left\{\frac{(1+Q_1)Q_3}{Q_1^2} + \frac{(1+Q_2)Q_4}{Q_2^2}\right\}, \tag{19}$$

where A is the Helmholtz free energy, P the pressure, and μ the chemical potential. Finally, s can be determined for given N, M, and T by minimizing the Helmholtz free energy, i.e. by solving the equation

$$0 = \frac{\partial}{\partial s}\left[\frac{A_c(s)}{NkT}\right]_{f,T} = 2(x-1)\ln\left(\frac{Q_2}{Q_1}\right) + 2\ln\left[\frac{s}{(1-2s)}\right] + \frac{2f}{xkT}\left(\frac{Q_5}{Q_1} + \frac{Q_6}{Q_2}\right) - \frac{2\left(1-\frac{1}{x}\right)fQ_3}{Q_1^2} + \frac{\left(1-\frac{1}{x}\right)fQ_4}{Q_2^2} \tag{20}$$

where $Q_5 = [(1+\delta)W_2 - W_1]2s + (W_1 - 2w_{ee})(1-2s)$

$Q_6 = [(\delta - 2)W_2 + w_{ee}]2s + [2(1-2\delta)W_2 + W_1](1-2s)$

More practically, one can determine f and s for given N, T and P by minimizing the Gibbs free energy. This can be done by solving (18) and (20) simultaneously, since, from thermodynamics,

$$\left(\frac{\partial G_c}{\partial s}\right)_{N,P,T} = \left(\frac{\partial A_c}{\partial s}\right)_{N,M,T}$$

At a particular pressure, the system can be shown to be isotropic (i.e., $s = \frac{1}{3}$ minimizes G_c) for sufficiently high T but anisotropic with nematic-like order ($s \ll \frac{1}{3}$) for lower temperatures. The transition temperature, the densities of the coexisting phases and the value of s in the anisotropic phase can be determined for the first-order nematic–isotropic transition at a particular pressure by solving the simultaneous equations

$$\Phi(f^{\mathrm{nem}}, s_{\mathrm{trans}}) = \frac{Pv_0}{kT_{\mathrm{trans}}} \tag{21}$$

$$\Phi(f^{\mathrm{iso}}, \tfrac{1}{3}) = \frac{Pv_0}{kT_{\mathrm{trans}}} \tag{22}$$

$$\mu\frac{(f^{\mathrm{nem}}, s_{\mathrm{trans}})}{kT_{\mathrm{trans}}} = \mu\frac{(f^{\mathrm{iso}}, \tfrac{1}{3})}{kT_{\mathrm{trans}}}, \tag{23}$$

where s_{trans} is the solution to (20) with $f = f^{\mathrm{nem}}$. Numerical results will be discussed in Section V.

B Smectic A Phase

In smectic A mesophases, the molecules are arranged in equidistant two-dimensional liquid layers with the preferred direction for their long axes normal to the plane of the layers. Unfortunately, the treatment of the last subsection does not apply to a system with such one-dimensional translational order since both Eqs. (10) and (14) were derived assuming the absence of any long range translational order. Moreover, given the rather severe translational and orientational restrictions imposed by the lattice, it does not seem feasible to derive a single partition function which will yield a smectic A mesophase as well as nematic and isotropic phases. Consequently, the lattice analog of the smectic A phase will be considered separately and its free energy then compared with those of the nematic and isotropic phases.

We shall assume that in the smectic A phase our N molecular rods are arranged on the lattice in parallel layers (with the center of every rod in a particular layer lying in precisely the same plane) and all point in the same direction, the direction normal to the planes of the layers. In principle, the $M - xN$ empty sites can occur in two kinds of positions: in layers of "holes" between layers of molecules and in vacancies in the latter (i.e. x adjacent empty sites where a rod is missing). In the thermodynamic limit, however, configurations containing layers of "holes" can be shown to make a vanishing contribution to ln Q_c. We shall assume, therefore, that all empty sites are located in the molecular layers. In this case, assuming the lattice to be a cubic array with edge length $M^{1/3}$, the number of layers $= M^{1/3}/x$, the number of rods per layer $= xN/M^{1/3}$, and the number of vacancies per layer $= M - xN/M^{1/3}$. Clearly, therefore,

$$\Omega(N, M) = \left[\frac{(M^{2/3})!}{\left(\frac{xN}{M^{1/3}}\right)!\left(\frac{M - xN}{M^{1/3}}\right)!}\right]^{\left(\frac{M^{1/3}}{x}\right)} \tag{24}$$

and

$$\bar{E}_c = \left(\frac{M^{1/3}}{x}\right)\left(\frac{xN}{M^{1/3}}\right)\{2[cw_{cc} + (x - c)w_{tt}] + w_{ee}\}\left(\frac{xN}{M}\right) \tag{25}$$

Furthermore,

$$\frac{A_c}{NkT} = \frac{-\ln Q_c}{N} = \frac{-\ln \Omega}{N} + \frac{\bar{E}_c}{NkT} = \ln f + \left(\frac{1}{f} - 1\right)\ln(1 - f) + \frac{f}{kT}\{2[cw_{cc} + (x - c)w_{tt}] + w_{ee}\} \tag{26}$$

$$\frac{S_c}{Nk} = \frac{\ln \Omega}{N} = \ln f + \left(\frac{1}{f} - 1\right)\ln(1 - f) \tag{27}$$

$$\Phi = \frac{Pv_0}{kT} = \left[\frac{\partial \ln Q_c}{\partial M}\right]_{N,T} = -\frac{1}{x}\ln(1 - f) + \frac{f^2}{xkT}\{2[cw_{cc} + (x - c)w_{tt}] + w_{ee}\} \tag{28}$$

and

$$\frac{\mu_c}{kT} = -\left[\frac{\partial \ln Q_c}{\partial N}\right]_{M,T} = \ln f - \ln(1 - f) + \frac{2f}{kT}\{2[cw_{cc} + (x - c)w_{tt}] + w_{ee}\} \tag{29}$$

Using (26), together with (16) and (20), one can compare the Helmholtz free energies of smectic A, nematic and isotropic phases at any f and T or, using (28), (29), (18), (19), and (20) one can compare Gibbs free energies at any fixed P and T. Such comparisons show that at sufficiently low T and high P or f, the smectic A arrangement is the stable one.

IV QUASI-CHEMICAL TREATMENT

In the Bragg-Williams approximation, the effect of the pair-wise intermolecular attractions on the configurational entropy of the system is not considered, or, in other words, correlations among the rods resulting from the attractive forces are completely neglected. This is frequently referred to as the zeroth approximation or zeroth order approximation. In this terminology, the first order approximation, or first improvement over the Bragg–Williams approach, is the quasi-chemical or Bethe–Guggenheim approximation, in which correlations between pairs of rod segments are considered, albeit rather crudely. When applied to the Ising model, the quasi-chemical approach yields significantly better results than does the Bragg–Williams approximation,[27] but this has often not been the case when both approaches have been applied to models of polymer solutions.[28] In order to test whether improved results can be obtained using the quasi-chemical approach, we have applied it to a special case of our lattice model; namely a system with

$$\begin{aligned} &w_{cc'} = w_{ct'} = w_{tt'} = w_\perp \\ &w_{cc} = w_{ct} = w_{tt} = w_{ee} = w_\parallel = \delta w_\perp \end{aligned} \tag{30}$$

In this case there is no longer any distinction between core and tail segments.

Applying the quasi-chemical approach necessitates considering rods in each of the three allowed orientations to be formally different species. Thus, the number of distinguishable ways in which a pair of directly adjacent sites, represented by $\underline{\quad}\,\underline{\quad}$, can be occupied are $\underline{0}\,\underline{0}$, $\underline{0}\,\underline{i}$, $\underline{i}\,\underline{0}$, $\underline{i}\,\underline{i}$, $\underline{j}\,\underline{k}$, and $\underline{k}\,\underline{j}$ $(i = 1, 2, 3;$ $j \leq 1 < k \leq 3)$ where 0 indicates an empty site and i, j, and k indicate occupation by a segment of a rod pointing in directions i, j, and k, respectively. Denoting by N_{00}, N_{0i}, etc. the number of pairs of sites of each type in a particular lattice configuration, we have the following "conservation" relations on a simple cubic lattice:

$$\begin{aligned} &2N_{00} + \sum_{i=1}^{3} (N_{0i} + N_{i0}) = 6(M - xN) \qquad (i = 1, 2, 3) \\ &2N_{ii} + N_{0i} + N_{i0} + \sum_{j \neq i} (N_{ij} + N_{ji}) = 6qN_i \end{aligned} \tag{31}$$

where

$$q = \frac{6x - 2x + 2}{6} = \frac{1}{3}(2x + 1);$$

that is, $6q$ is the number of nearest neighbor sites to the x segments of a rod excluding those sites occupied by an adjoining segment of the same rod. We shall choose the N_{0i}, N_{i0}, and $N_{ij}(i \neq j)$ as independent variables and obtain N_{00} and the N_{ii} from (31). The configurational partition function for the system can then be written

$$Q_c = \sum_{\mathbf{N}_{mn}} g(M, \mathbf{N}_i, \mathbf{N}_{mn}) \exp(-E_c(\mathbf{N}_{mn}, w_\parallel, w_\perp)/kT) \tag{32}$$

where $\mathbf{N}_i$ represents the set $\{N_1^*, N_2^*, N_3^*\}$ which maximizes $Q_c(\mathbf{N}_i)$; $\mathbf{N}_{mn}$ represents the set $\{N_{0i}, N_{i0}, N_{ij}\}(i \neq j)$; and g is the number of ways of placing $N_1^* + N_2^* + N_3^*$ rods, in their respective orientations, on the lattice such that there are N_{01}, $\underline{0}\ \underline{1}$ pairs, N_{10} $\underline{1}\ \underline{0}$ pairs, ..., N_{32} $\underline{3}\ \underline{2}$ pairs. Clearly

$$\begin{aligned} E_c(\mathbf{N}_{mn}, w_{\parallel}, w_{\perp}) &= \sum_{i=1}^{3} N_{ii} w_{\parallel} + \sum_{i \neq j} N_{ij} w_{\perp} \\ &= \left[(2x + 1)N - \frac{1}{2}\sum_{i=1}^{3}(N_{0i} + N_{i0}) - \sum_{i \neq j}\sum N_{ij}\right] w_{\parallel} \\ &\quad + \sum_{i \neq j}\sum N_{ij} w_{\perp} \end{aligned} \tag{33}$$

The essence of the quasi-chemical approximation is that pairs of neighboring sites can, in a sense, be treated as independent entities. In the combinatorial approach used here, which is an extension of that of Fowler and Guggenheim,[29] one calculates $\omega(M, \mathbf{N}_i^*, \mathbf{N}_{mn})$, the number of ways of randomly permuting N_{01}, $\underline{0}\ \underline{1}$ pairs, ..., N_{32} $\underline{3}\ \underline{2}$ pairs, assuming complete independence for all pairs, and then assumes that g is equal to ω except for a normalization factor C; i.e., one lets

$$g(M, \mathbf{N}_i^*, \mathbf{N}_{mn}) = C(M, \mathbf{N}_i^*)\omega(M, \mathbf{N}_i^*, \mathbf{N}_{mn}) \tag{34}$$

(Clearly, C will be $\ll 1$ since many physically impossible configurations are counted in ω. What is being assumed is that all types of pairs are being overcounted to the same extent in ω). From elementary combinatorics,

$$\omega(M, \mathbf{N}_i^*, \mathbf{N}_{mn}) = \frac{[N_{00} + \sum_{i=1}^{3}(N_{0i} + N_{i0}) + \sum_{i=1}^{3} N_{ii} + \sum\sum_{i \neq j} N_{ij}]!}{N_{00}!\prod_{i=1}^{3}[N_{0i}!N_{i0}!N_{ii}!]\prod_{i,j;i \neq j}[N_{ij}!]} \tag{35}$$

Utilizing (31), this becomes

$$\begin{aligned} \omega = {} & [3(M - (x - q)N)]!\left\{\left[3(M - xN) - \frac{1}{2}\sum_{i=1}^{3}(N_{0i} + N_{i0})\right]!\right\}^{-1} \\ & \cdot\left\{\left[\prod_{i=1}^{3}\left(\left[3qN_i^* - \frac{1}{2}(N_{0i} + N_{i0}) - \sum_{j \neq i} N_{ij}\right]! N_{0i}! N_{i0}!\right)\right]\left[\prod_{\substack{i,j \\ i \neq j}}(N_{ij}!)\right]\right\}^{-1} \end{aligned}$$

C can be determined from the normalization condition

$$C(M, \mathbf{N}_i^*) \sum_{N_{mn}} \omega(M, \mathbf{N}_i^*, \mathbf{N}_{mn}) = \sum_{N_{mn}} g(M, \mathbf{N}_i^*, \mathbf{N}_{mn}) = \Omega(M, \mathbf{N}_i^*), \tag{37}$$

where Ω is given by (10).

In the thermodynamic limit, the sum over $\mathbf{N}_{mn}$ can be replaced by its maximum term. Then, taking natural logarithms, evaluating $\ln \omega_{\max}$, and simplifying one obtains

$$\ln C = \ln \Omega + 6(M - xN)\ln\left\{\frac{M - xN}{M - (x - q)N}\right\} + \sum_{i=1}^{3} 6qN_i^* \ln\left\{\frac{qN_i^*}{M - (x - q)N}\right\} \tag{38}$$

or

$$C = \frac{1}{(M!)^2(M - xN)!}\left\{\prod_{i=1}^{3}\left(\frac{[M - (x - 1)N_i^*]!(qN_i^*)^{6qN_i^*}}{N_i^*!}\right)\right\} \cdot \left\{\frac{(M - xN)^{(M - xN)}}{[M - (x - q)N]^{[M - (x - q)N]}}\right\}^6 \tag{39}$$

Finally, substituting g obtained from (39), (36), and (34) into (32), replacing the sum over $\mathbf{N}_{mn}$ by its maximum term, and taking the logarithm of Q_c gives

$$\begin{aligned}\ln Q_c = {} & \sum_{i=1}^{3} [M - (x - 1)N_i^*]\ln[M - (x - 1)N_i^*] - 2M \ln M \\ & + 5(M - xn)\ln(M - xN) + (4x + 1) \sum_i N_i^* \ln N_i^* \\ & - 3\left[M - (x - 1)\frac{N}{3}\right]\ln\left[M - (x - 1)\frac{N}{3}\right] + 2(2x + 1)N \ln\left[\frac{2x + 1}{3}\right] \\ & - \sum_i \left[\bar{N}_{0i} \ln\left(\frac{\bar{N}_{0i}}{3}\right) + \bar{N}_{i0} \ln\left(\frac{\bar{N}_{i0}}{3}\right)\right] - \sum_{i \neq j}\sum \bar{N}_{ij} \ln\left(\frac{N_{ij}}{3}\right)\end{aligned}$$

$$-3\left[M - xN - \frac{1}{6}\sum_{i=1}^{3}(\bar{N}_{0i} + \bar{N}_{i0})\right]\ln\left[M - xN - \frac{1}{6}\sum_{i}(\bar{N}_{0i} + \bar{N}_{i0})\right]$$

$$-3\sum_{i=1}^{3}\left[qN_i^* - \frac{1}{6}(\bar{N}_{0i} + \bar{N}_{i0}) - \frac{1}{3}\sum_{j\neq i}\bar{N}_{ij}\right]$$

$$\cdot\ln\left[qN_i^* - \frac{1}{6}(\bar{N}_{0i} + \bar{N}_{i0}) - \sum_{j\neq i}\bar{N}_{ij}\right]$$

$$-\frac{1}{kT}\left\{\left[(2x + 1)N - \frac{1}{2}\sum_{i}(\bar{N}_{0i} + \bar{N}_{i0})\right]w_{\parallel} + \sum_{i\neq j}\bar{N}_{ij}(w_{\perp} - w_{\parallel})\right\}, \tag{40}$$

where the set $\bar{N}_{mn}$ is the solution to the so-called quasi-chemical equations:

$$\frac{4\bar{N}_{0i}^2}{[6(M - xN) - \sum_k(\bar{N}_{0k} + \bar{N}_{k0})][2(2x + 1)N_i^* - \bar{N}_{i0} - \bar{N}_{0i} - \sum_{l\neq 1}(\bar{N}_{il} + \bar{N}_{li})]} = \exp\left(\frac{w_{\parallel}}{kT}\right)$$

$$\frac{4\bar{N}_{i0}^2}{[6(M - xN) - \sum_k(\bar{N}_{0k} + \bar{N}_{k0})][2(2x + 1)N_i^* - \bar{N}_{i0} - \bar{N}_{0i} - \sum_{l\neq i}(\bar{N}_{il} + \bar{N}_{li})]} = \exp\left(\frac{w_{\parallel}}{kT}\right)\begin{bmatrix} i, j = 1, 2, 3 \\ i \neq j \end{bmatrix}$$

$$\frac{4\bar{N}_{ij}^2}{[2(2x+1)N_i^* - \bar{N}_{i0} - \bar{N}_{0i} - \sum_{l\neq i}(\bar{N}_{il} + \bar{N}_{li})][2(2x+1)N_j^* - \bar{N}_{j0} - \bar{N}_{0j} - \sum_{k\neq j}(\bar{N}_{jk} + \bar{N}} = \exp\left[\frac{2(w_{\parallel} - w_{\perp}}{kT}\right] \tag{41}$$

derived by maximizing the function ln $Q_c(\mathbf{N}_{mn})$ with respect to $\mathbf{N}_{mn}$. From (41) it is clear that

$$\begin{aligned} \bar{N}_{0i} &= \bar{N}_{i0} \quad (\text{all } i \text{ and } j) \\ \bar{N}_{ij} &= \bar{N}_{ji} \end{aligned} \tag{42}$$

Moreover, again singling out direction 1 as the preferred direction and assuming that $N_2^* = N_3^*$, we see that

$$\begin{aligned} \bar{N}_{02} &= \bar{N}_{20} = \bar{N}_{03} = \bar{N}_{30} \\ \bar{N}_{12} &= \bar{N}_{21} = \bar{N}_{13} = \bar{N}_{31}. \end{aligned} \tag{43}$$

Making use of (42) and (43) and introducing reduced variables, (40) and (41) become respectively,

$$\begin{aligned}
\frac{-\ln Q_c}{N} = \frac{A_c}{NkT} = \frac{x}{f}\Bigg\{ & -5(1-f)\ln(1-f) \\
& + 3\left[1-\left(1-\frac{1}{x}\right)\frac{f}{3}\right]\ln\left[1-\left(1-\frac{1}{x}\right)\frac{f}{3}\right] \\
& + 6[\eta_{01}\ln\eta_{01} + 2\eta_{02}\ln\eta_{02} + 2\eta_{12}\ln\eta_{12} + \eta_{23}\ln\eta_{23}] \\
& + 3[1 - f - \eta_{01} - 2\eta_{02}]\ln[1 - f - \eta_{01} - 2\eta_{02}] \\
& + 3\left[\left(2+\frac{1}{x}\right)(1-2s)\frac{f}{3} - \eta_{01} - 2\eta_{12}\right] \\
& \cdot \ln\left[\left(2+\frac{1}{x}\right)(1-2s)\frac{f}{3} - \eta_{01} - 2\eta_{12}\right] \\
& + 6\left[\left(2+\frac{1}{x}\right)s\frac{f}{3} - \eta_{02} - \eta_{12} - \eta_{23}\right] \\
& \cdot \ln\left[\left(2+\frac{1}{x}\right)s\frac{f}{3} - \eta_{02} - \eta_{12} - \eta_{23}\right] \\
& - \left[1-\left(1-\frac{1}{x}\right)(1-2s)f\right]\ln\left[1-\left(1-\frac{1}{x}\right)(1-2s)f\right] \\
& - 2\left[1-\left(1-\frac{1}{x}\right)sf\right]\ln\left[1-\left(1-\frac{1}{x}\right)sf\right]\Bigg\} \\
& - 2(2x+1)\ln\left[\frac{2x+1}{3}\right] \\
& - (4x+1)\left\{(1-2s)\ln(1-2s) + 2s\ln s + \ln\left(\frac{f}{x}\right)\right\} \\
& + \frac{x}{fkT}\Bigg\{\left[\left(2+\frac{1}{x}\right)f - 3\eta_{01} - 6\eta_{02}\right]w_{\parallel} \\
& + 6(2\eta_{12} + \eta_{23})(w_{\perp} - w_{\parallel})\Bigg\} \qquad (44)
\end{aligned}$$

and

$$\frac{\eta_{01}^{2}}{[1-f-\eta_{01}-2\eta_{02}]\left[\left(2+\dfrac{1}{x}\right)(1-2s)\dfrac{f}{3}-\eta_{01}-2\eta_{12}\right]}=\exp\left(\frac{w_{\parallel}}{kT}\right)$$

$$\frac{\eta_{02}^{2}}{[1-f-\eta_{01}-2\eta_{02}]\left[\left(2+\dfrac{1}{x}\right)s\dfrac{f}{3}-\eta_{02}-\eta_{12}-\eta_{23}\right]}=\exp\left(\frac{w_{\parallel}}{kT}\right)$$

$$\frac{\eta_{12}^{2}}{\left[\left(2+\dfrac{1}{x}\right)(1-2s)\dfrac{f}{3}-\eta_{01}-2\eta_{12}\right]\left[\left(2+\dfrac{1}{x}\right)s\dfrac{f}{3}-\eta_{02}-\eta_{12}-\eta_{23}\right]}$$

$$=\exp\left[\frac{2(w_{\parallel}-w_{\perp})}{kT}\right]$$

$$\frac{\eta_{23}^{2}}{\left[\left(2+\dfrac{1}{x}\right)s\dfrac{f}{3}-\eta_{02}-\eta_{12}-\eta_{23}\right]^{2}}=\exp\left[\frac{2(w_{\parallel}-w_{\perp})}{kT}\right] \tag{45}$$

where

$$\eta_{mn}=\frac{\bar{N}_{mn}}{3M} \tag{46}$$

and s and f are defined in (13).

This set of simultaneous equations can be solved partially to give

$$\eta_{01}=\frac{[1+e^{-w/kT}]\eta_{02}\eta_{12}}{\left(2+\dfrac{1}{x}\right)s\dfrac{f}{3}-\eta_{02}-\eta_{12}} \tag{47a}$$

$$\eta_{23}=\frac{\left(2+\dfrac{1}{x}\right)s\dfrac{f}{3}-\eta_{02}-\eta_{12}}{[1+e^{-(w/kT)}]} \tag{47b}$$

$$2\eta_{02}=1-f-\frac{\eta_{02}[1+e^{-w/kT}][\eta_{12}+e^{-w_{\perp}/kT}\eta_{02}]}{\left(2+\dfrac{1}{x}\right)s\dfrac{f}{3}-\eta_{02}-\eta_{12}} \tag{47c}$$

$$2\eta_{12}=\left(2+\frac{1}{x}\right)(1-2s)\frac{f}{3}-\frac{\eta_{12}[1+e^{-w/kT}][\eta_{02}+e^{-w/kT}\eta_{12}]}{\left(2+\dfrac{1}{x}\right)s\dfrac{f}{3}-\eta_{02}-\eta_{12}} \tag{47d}$$

where

$$w = w_{\parallel} - w_{\perp} = (\delta - 1)w_{\perp}$$

(47c) and (47d) can be solved iteratively for η_{12} and η_{02}, then η_{01} and η_{23} obtained from (47a) and (47b). Finally, s can be determined from the maximization condition

$$\begin{aligned} 0 = \left(\frac{\partial \ln Q_c}{\partial s}\right)_{f,T} &= \left(\frac{\partial \ln Q_c}{\partial s}\right)_{f,T,N_{mn}} + \sum_{i=1}^{3} \left(\frac{\partial \ln Q_c}{\partial \overline{N}_{0i}}\right)_{f,T,s} \left(\frac{\partial \overline{N}_{0i}}{\partial s}\right)_{f,T} \\ &\quad + \sum_{i \neq j} \left(\frac{\partial \ln Q_c}{\partial N_{ij}}\right)_{f,T,s} \left(\frac{\partial \overline{N}_{ij}}{\partial s}\right)_{f,T} \\ &= -2(x-1)\ln\left(\frac{Q_2}{Q_1}\right) + 2(4x+1)\ln\left(\frac{s}{1-2s}\right) \\ &\quad - 2(2x+1)\ln\left[\frac{\left(2+\frac{1}{x}\right)s\frac{f}{3} - \eta_{02} - \eta_{12} - \eta_{23}}{\left(2+\frac{1}{x}\right)(1-2s)\frac{f}{3} - \eta_{01} - 2\eta_{12}}\right] \end{aligned} \tag*{48)}$$

since $(\partial \ln Q_c/\partial N_{0i})_{f,T,s}$ and $(\partial \ln Q_c/\partial N_{ij})_{f,T,s}$ vanish.

The values of f, s, η_{12}, and η_{02} can be determined for any given P and T by simultaneously solving (47) and (48), together with

$$\begin{aligned} \Phi = \frac{Pv_0}{kT} = \left(\frac{\partial \ln Q_c}{\partial M}\right)_{N,T} &= 5\ln(1-f) - 3\ln\left[1 - \left(1 - \frac{1}{x}\right)\frac{f}{3}\right] \\ &\quad - 3\ln[1 - f - \eta_{01} - 2\eta_{02}] + \ln\left[1 - \left(1 - \frac{1}{x}\right)(1-2s)f\right] \\ &\quad + 2\ln\left[1 - \left(1 - \frac{1}{x}\right)sf\right]. \end{aligned} \tag{49}$$

In the next section, numerical results will be presented and compared with those obtained in the Bragg–Williams approximation.

V RESULTS

In this section, the behavior of our model system will be presented. Of primary interest—both intrinsically and with respect to comparison with experimental data—are the relative stabilities of the smectic A, nematic, and isotropic phases, as reflected in the smectic → nematic and nematic → isotropic transition temperatures, and the nature of these phase transitions.

A Bragg–Williams Results

At this point, our model parameters are the segment volume v_0, the molecular length-to-breadth ratio x, the segmental attractive energies $w_{cc'}$, $w_{ct'}$, $w_{tt'}$, w_{ee}, and the anisotropy factor δ. (See (15)). Since the numerical results can be shown to be quite insensitive to the precise value of w_{ee}, it will be assumed that

$$w_{ee} = w_{tt} = \delta w_{tt'}. \tag{50}$$

Finally, we shall also make the assumption, traditional in lattice and cell theories, that

$$w_{ct'} = \sqrt{w_{cc'} w_{tt'}}, \tag{51}$$

leaving us with the five parameters v_0, x, δ, $w_{cc'}$, and $w_{tt'}$, in addition to the independent thermodynamic variables P and T.

From the heat of vaporization and molecular dimensions of *p*-azoxyanisole (PAA), for which we assume $x \approx 3$, it would appear that $w_{cc'}/k$ should be of order -1000 K while Pv_0/k should be of order 1 K near atmospheric pressure. When such values are used, however, quite "pathological" behavior ensues; namely, the system is smectic and quite dense up to very high temperatures (of order 1000 K), then undergoes a first order transition to an isotropic gas! (f values of order 0.01). In order to obtain a stable nematic phase, reasonable smectic → nematic (S → N) and nematic → isotropic (N → I) transition temperatures, and isotropic phases with densities of the same order of magnitude as the corresponding nematic phases, it is necessary to decrease $w_{cc'}/k$ by roughly an order of magnitude while increasing Pv_0/k by somewhat more than an order of magnitude. Even then, the results are disappointing, at least with respect to the nematic → isotropic transition, as can be seen from Figures 3 and 4,[30] where the dependence of the properties of that transition on the molecular length-to-breadth ratio x and the anisotropy factor δ is summarized for systems with $c = 3$, $w_{tt'}/k = -40$ K, $w_{cc'} = 3w_{tt'}$, and $Pv_0/k = 30$ K. Clearly, the behavior shown bears scant resemblance to that exhibited by homologous series of nematogens, along which the N → I transition temperatures slowly decrease and the entropies of transition rapidly increase as the molecular "tails" are lengthened, while the relative density discontinuity $(\rho_{\text{nem}} - \rho_{\text{iso}})/\rho_{\text{nem}}$ is commonly less than one percent. Experimentally measured[31] nematic order parameters η, defined by

$$\eta = \left\langle \left(\frac{3}{2} \cos^2 \theta - \frac{1}{2} \right) \right\rangle, \tag{52}$$

where θ is the angle between the long axis of a molecule and the preferred direction and the brackets denote the average value, are typically in the

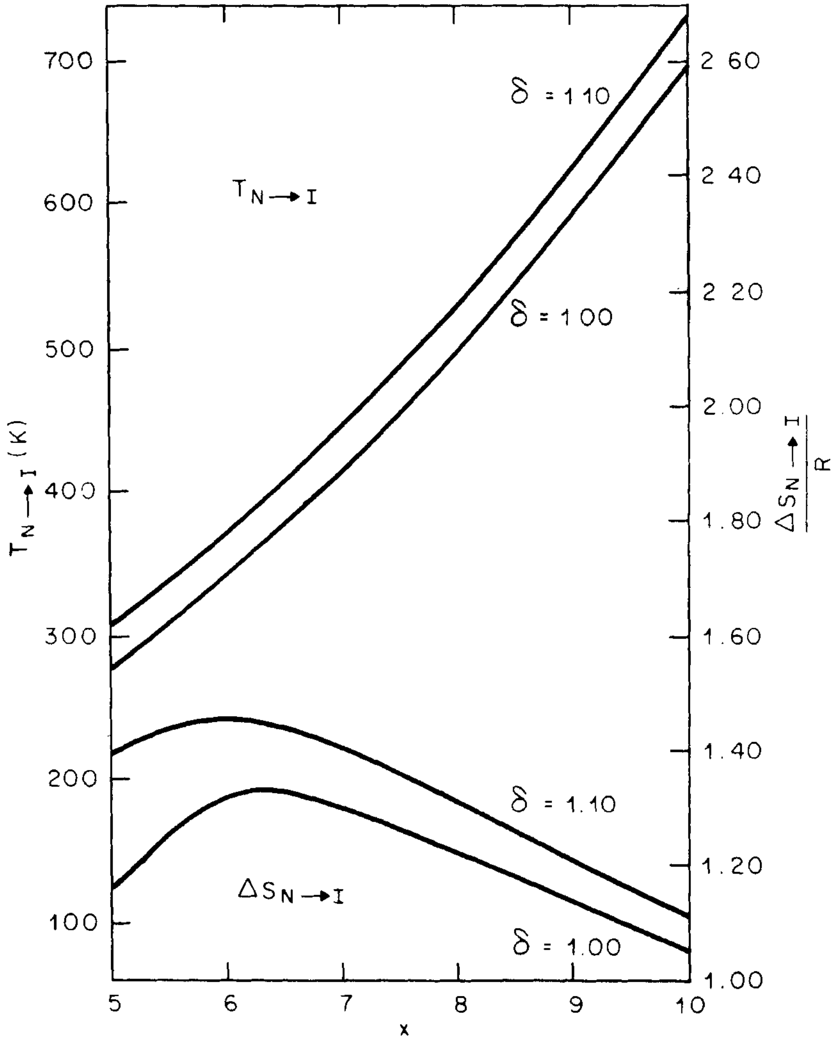

FIGURE 3 The nematic → isotropic transition temperature $T_{N\to I}$ and entropy of transition $\Delta S_{N\to I}$ as functions of the rod length to-breadth ratio x.

$$\frac{w_{tt'}}{k} = -40\text{ K}, \quad \frac{Pv_0}{k} = 30\text{ K}, \quad \frac{w_{cc'}}{w_{tt'}} = 3, \quad \text{and} \quad \delta = \frac{w_{cc}}{w_{cc'}} = \frac{w_{ct}}{w_{ct'}} = \frac{w_{tt}}{w_{tt'}}.$$

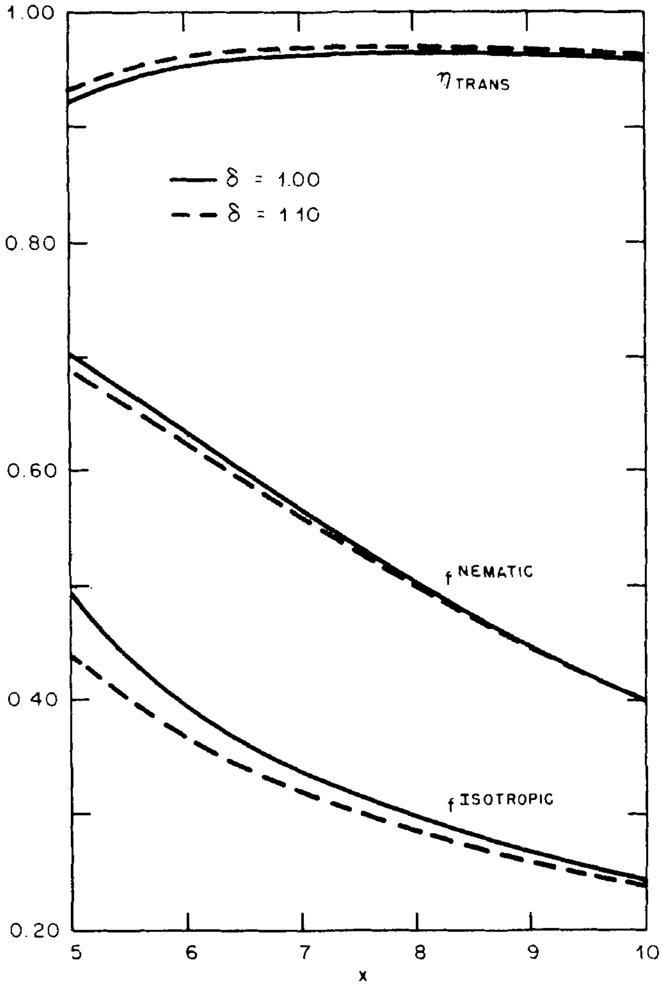

FIGURE 4 The dimensionless densities f^{nematic} and $f^{\text{isotropic}}$ and the order parameter η_{trans} at the nematic → isotropic transition as functions of the rod length-to-breadth ratio x. The various model parameters have the same values as in Figure 3.

range 0.3 to 0.5 near the N → I transition temperature. For the model system,

$$\eta = \frac{3}{2}\left[(1 - 2s)\cos^2 0 + 2s\cos^2\left(\frac{\Pi}{2}\right)\right] - \frac{1}{2} = 1 - 3s. \qquad (53)$$

The fact that the predicted N → I transition temperatures increase with increasing x, even when the tail–tail interactions are much weaker than core–

core interactions, provides additional evidence[10] that the experimentally observed decrease in $T_{N\rightarrow I}$ along homologous series result primarily from the increasing flexibility of the hydrocarbon end-chains. Otherwise, the lattice model seems to be of little use for investigating the nematic → isotropic phase transition.

The behavior of the smectic A → nematic transition for the lattice model is summarized in Figures 5 and 6 and Table I, while Figure 7 is included to illustrate that it is not really possible to choose a set of parameters: Pv_0/k, $w_{tt'}/k$, and $w_{cc'}/w_{tt'}$ which will yield both realistic S → N and N → I transition temperatures. (For the systems represented in Figures 5 and 6, the N → I transition temperatures are much too high.) As can be seen, both the transition temperature and the entropy of transition increase as the "tail" portions of the rods are lengthened, increasing relatively rapidly at first, then levelling off for longer rods. Qualitatively, this is a type of behavior frequently observed in homologous series exhibiting smectic and nematic or cholesteric mesophases, although in the real systems, the levelling off usually is accompanied by the merging of the S → N and N → I transition temperature curves to form the smectic A → isotropic transition temperature curve. (This does not occur with the lattice model because $T_{N\rightarrow I}$ increases rapidly with increasing x). In other homologous series, the S → N transition temperatures at first increase as methylene groups are added to the "tails" then pass through a maximum and begin to decrease. These decreases in $T_{S\rightarrow N}$ probably result—as do the commonly observed decreases in $T_{N\rightarrow I}$—from the increasing flexibility of the molecular end chains and would not be expected to occur in a system of inflexible rods. Quantitatively, the calculated values of ΔS_{trans} are too large by factors of perhaps 3 to 5 and increase too slowly with increasing rod length. In addition, the densities of both phases near the transition are unphysically large; the orientational order in the nematic phase is much too high; and the relative density discontinuities are too large by somewhat less than an order of magnitude. (The large density discontinuities are probably the major "cause" of the large values of ΔS_{trans}.) Nevertheless, the agreement between the model behavior and experiment is clearly much better here than was the case for the nematic → isotropic transition. That reasonable results were obtained despite the crude treatment of the smectic A phase (constrained to have perfect orientational and 1-dimensional translational order) encourages one to hope that more sophisticated lattice and cell models might prove useful for studying the relative stabilities of the nematic and various smectic mesophases. Such improved models will be discussed briefly in Section VI.

Clearly, for a fixed value of x, the S → N transition temperature is increased by increasing δ, $w_{cc'}/w_{tt'}$, or $w_{tt'}$ (holding $w_{cc'}/w_{tt'}$ fixed). In order to obtain a stable smectic phase and a reasonable $T_{S\rightarrow N}$, w_{cc} must be considerably

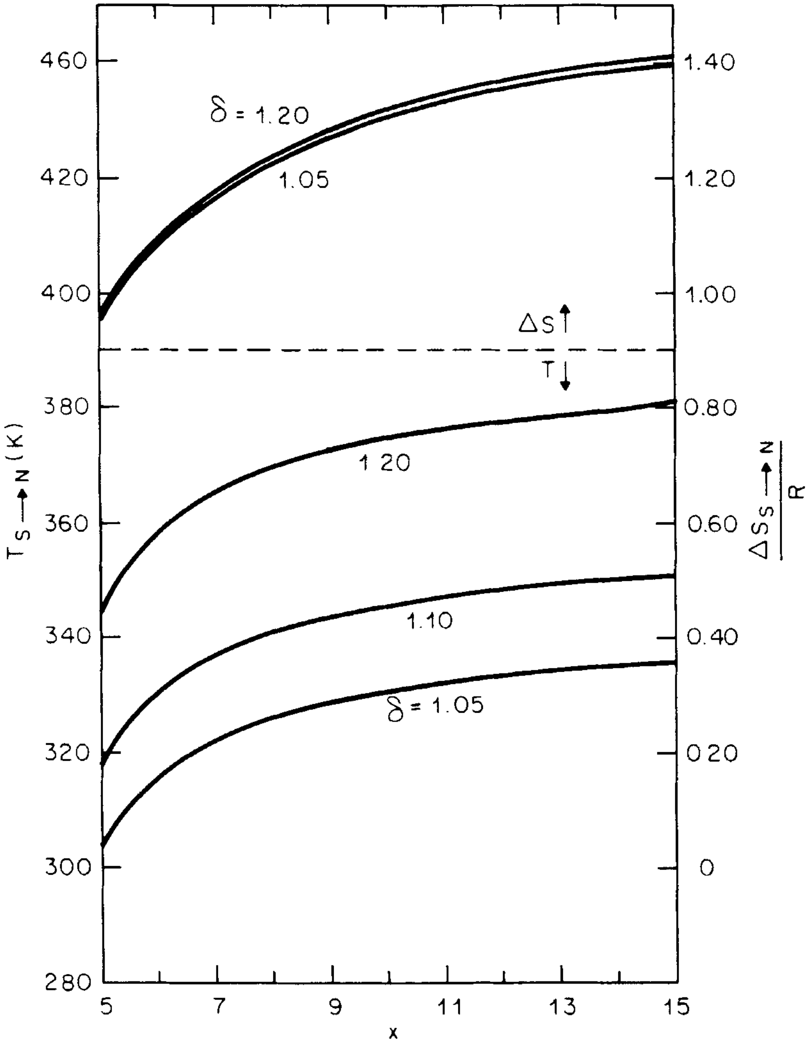

FIGURE 5 The smectic A → nematic transition temperature $T_{S \to N}$ and entropy of transition $\Delta S_{S \to N}$ as functions of the rod length-to-breadth ratio x for several values of the anisotropy parameter δ. In all cases,

$$\frac{w_{tt'}}{k} = -75\ \mathrm{K}, \quad \frac{Pv_0}{k} = 30\ \mathrm{K}, \quad \text{and} \quad \frac{w_{cc'}}{w_{tt'}} = 3.$$

(The entropy curve for $\delta = 1.10$ has been omitted for purposes of clarity. It lies between those for $\delta = 1.20$ and $\delta = 1.05$.)

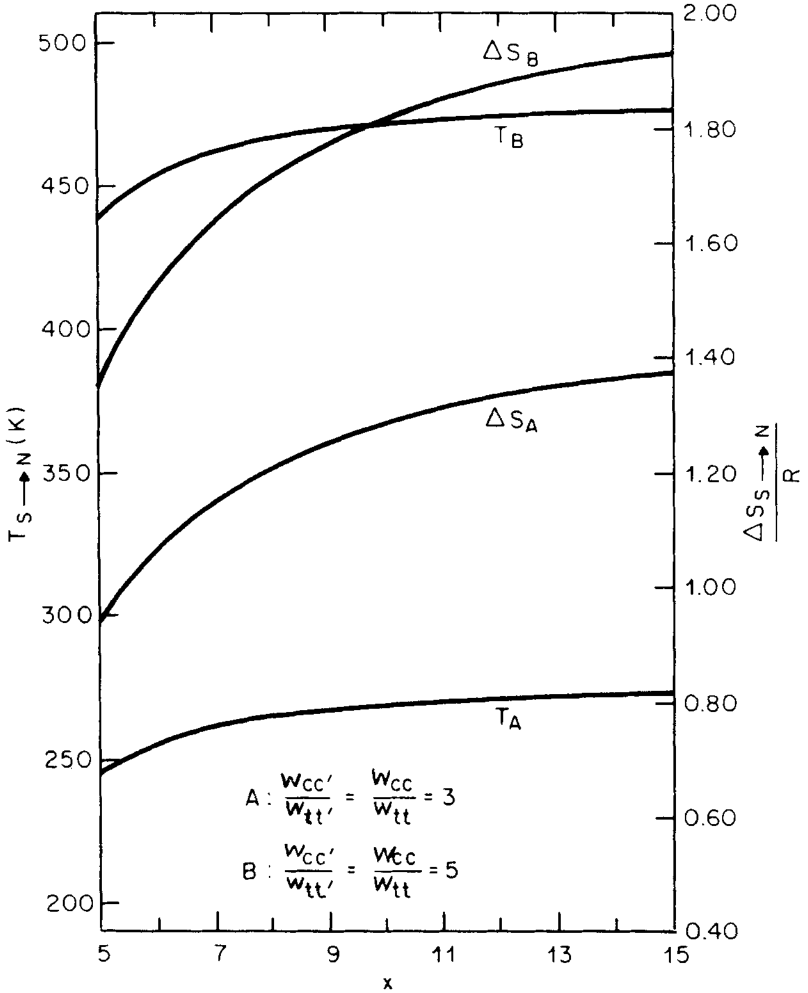

FIGURE 6 The smectic A → nematic transition temperature $T_{S \to N}$ and entropy of transition $\Delta S_{S \to N}$ as functions of the rod length-to-breadth ratio x at two values of the ratio $w_{cc'}/w_{tt'} = w_{cc}/w_{tt}$. In both instances,

$$\frac{w_{tt'}}{k} = -60\text{ K}, \quad \frac{Pv_0}{k} = 30\text{ K}, \quad \text{and} \quad \delta = 1.05.$$

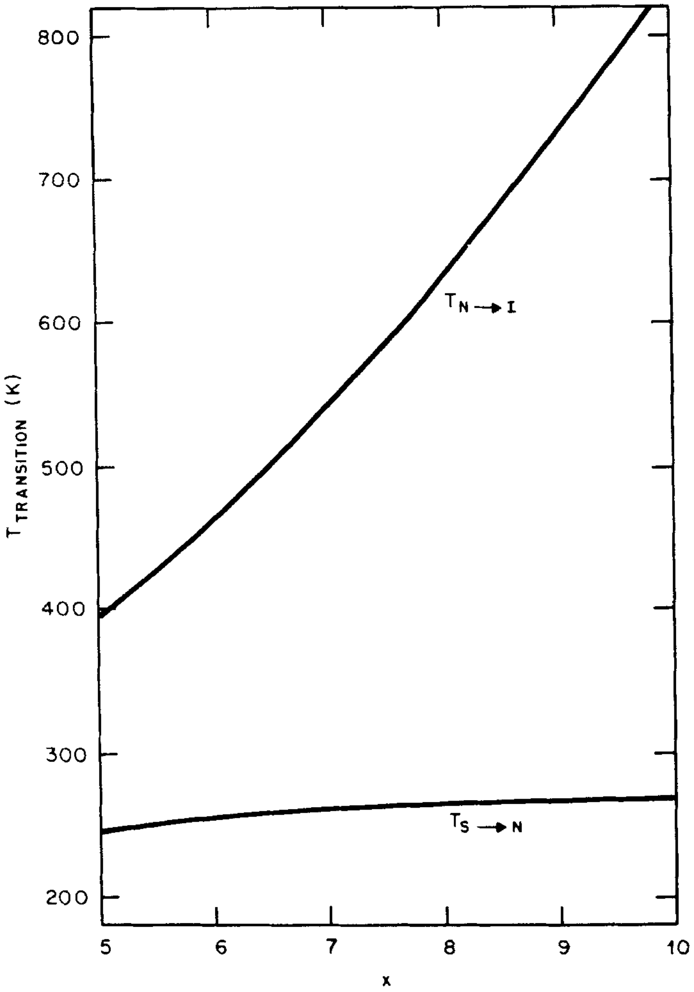

FIGURE 7 The smectic A → nematic (S → N) and nematic → isotropic (N → I) transition temperatures as functions of the rod length-to-breadth ratio x when

$$\frac{w_{tt}}{k} = -60\ \text{K}, \quad \frac{Pv_0}{k} = 30\ \text{K}, \quad \frac{w_{cc'}}{w_{tt'}} = 3, \quad \text{and} \quad \delta = 1.05.$$

TABLE I

Dimensionless densities (f^{sm} and f^{nem}) and relative density discontinuities ($\Delta f/f^{sm}$) at the smectic A → nematic transition for several systems. In all cases, $Pv_0/k = 30$ K and $\eta_{trans} > 0.99$ for the nematic phase.

	$\frac{w_{tt'}}{k} = -75$ K		$\frac{w_{cc'}}{w_{tt'}} = 3$	$\frac{w_{tt'}}{k} = -75$ K		$\frac{w_{cc'}}{w_{tt'}} = 3$	$\frac{w_{tt'}}{k} = -60$ K		$\frac{w_{cc'}}{w_{tt'}} = 3$	$\frac{w_{cc'}}{k} = -60$ K		$\frac{w_{cc'}}{w_{tt'}} = 5$
		$\delta = 1.05$			$\delta = 1.20$			$\delta = 1.05$			$\delta = 1.05$	
x	f^{sm}	f^{nem}	$\Delta f/f^{sm}$	f^{sm}	f^{nem}	$\Delta f/f^{sm}$	f^{sm}	f^{nem}	$\Delta f/f^{sm}$	f^{sm}	f^{nem}	$\Delta f/f^{sm}$
5	0.998	0.908	0.090	0.998	0.907	0.091	0.998	0.911	0.088	0.995	0.837	0.159
7	0.999	0.906	0.087	0.999	0.905	0.094	0.999	0.908	0.092	0.997	0.828	0.169
9	0.9997	0.914	0.086	0.9997	0.913	0.087	0.9998	0.916	0.083	0.998	0.840	0.158
11	0.9999	0.923	0.077	0.9999	0.922	0.078	0.9999	0.925	0.075	0.999	0.854	0.145
13	0.99997	0.930	0.070	0.99997	0.929	0.071	0.99997	0.932	0.068	0.9995	0.867	0.132
15	0.99999	0.937	0.063	0.99999	0.935	0.064	0.99999	0.939	0.061	0.9997	0.879	0.119

larger than w_{tt}, in agreement with the observation of Gray[32] that strongly attracting molecular "cores" seem to be a *sine qua non* for the occurrence of smectic ordering. Contrary to Gray's suppositions, however, such strong core–core attractions do not result from the direct interaction between aligned transverse group dipoles since it is now established[33] that there is free rotation about the molecular long axes in smectic A mesophases.

B Quasi-Chemical Results

Numerical results obtained in the quasi-chemical approximation are presented and compared with Bragg–Williams results in Figure 8 and Table II. Only the behavior near the nematic → isotropic transition is shown, since there is no stable smectic A phase when $w_{cc'} = w_{tt'}$. As can be seen, the densities of both phases at the transition are higher and the transition temperatures are lower and increase less rapidly with increasing x in the quasi-chemical approximation than in the Bragg–Williams approximation. On the other hand, the quasi-chemical values of η_{trans}, Δf_{trans}, and ΔS_{trans} are higher than the corresponding Bragg–Williams values. Overall, the quasi-chemical results are just as poor as the Bragg–Williams results,[34] and the quasi-chemical approach has, therefore, not been pursued further.

The quasi-chemical results just discussed, as well as the derivations of Section IV are, in a sense, a correction to Reference 20, where a face-centered cubic (fcc) lattice containing N_x hard inflexible rods of length-to-breadth ratio x and N_0 "solute molecules" (each occupying a single site), with segmental attractive energies w_{00}, w_{0x}, w_{xx} (interacting segments on parallel rods), and $w_{xx'}$ (interacting segments on non-parallel rods), was treated in the quasi-chemical approximation. The configurational partition function

TABLE II

Comparisons of nematic order parameters (η_{trans}), dimensionless densities (f^{nem} and f^{iso}), and relative density discontinuities ($\Delta f/f^{\text{nem}}$) at the nematic → isotropic phase transition obtained in the quasi-chemical and in the Bragg–Williams approximations. For the systems considered, $w_{\perp}/k = -75$ K, $Pv_0/k = 30$ K, and $\delta = 1.05$.

	Quasi-chemical approximation				Bragg–Williams approximation			
x	η_{trans}	f^{nem}	f^{iso}	$\Delta f/f^{\text{nem}}$	η_{trans}	f^{nem}	f^{iso}	$\Delta f/f^{\text{nem}}$
5	0.948	0.797	0.543	0.319	0.919	0.715	0.498	0.304
6	0.978	0.745	0.424	0.431	0.958	0.645	0.386	0.402
7	0.988	0.693	0.357	0.485	0.972	0.584	0.325	0.443
8	0.991	0.639	0.313	0.510	0.976	0.528	0.285	0.460
9	0.991	0.579	0.280	0.516	0.977	0.475	0.256	0.463
10	0.990	0.517	0.254	0.508	0.976	0.429	0.233	0.457

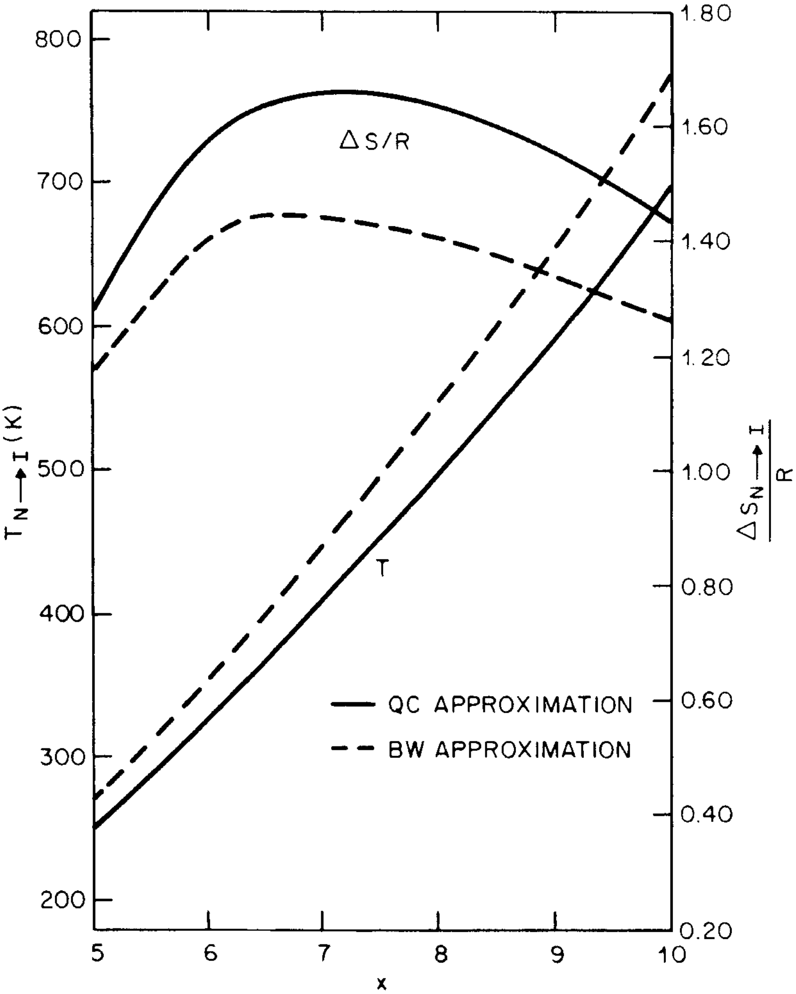

FIGURE 8 A comparison of the Bragg–Williams and Quasi-chemical approximations.

$$\frac{w_{\perp}}{k} = -75 \text{ K}, \quad \frac{Pv_0}{k} = 30 \text{ K}, \quad \delta = 1.05.$$

derived therein (Eq. 18) is correct, as are the expression for the configurational energy (Eq. 19) and the quasi-chemical equations (Eqs. 20). In fact, in the special case $w_{00} = w_{0x} = 0$ (i.e., a lattice of rods and empty sites or "holes") these equations can be shown to be identical to (40) and (41) of the present work except that one sums over six rather than three allowed orientations with an fcc lattice. Subsequent to the derivation of (18) to (20) and the specialization to a system of rods and "holes" (the only case for which numerical results were obtained), however, two errors were made in the earlier paper. First, it was mistakenly concluded that in the anisotropic phase, the system is perfectly ordered orientationally at all temperatures and densities, whereas, in reality, the distribution $N_1 = N_x$; $N_2 = N_3 = N_4 = N_5 = N_6 = 0$ minimizes the free energy only in the close-packed limit. More seriously, PV effects were neglected with the result that

1) temperature and density are both independent variables;
2) $G_c = A_c$ and $H_c = E_c$ (H is the enthalpy);
3) the anisotropic → isotropic phase transition occurs at constant density.

These errors—particularly the second one—are sufficiently serious to invalidate many of the conclusions drawn by the authors. In particular, it is *not* true that the model can explain the trends in the nematic → isotropic transition temperature and entropy of transition along homologous series of nematogens. Rather, the behavior of the fcc system should be very similar to that of the simple cubic system considered here in all respects, including the dependence of T_{trans} and ΔS_{trans} on the length-to-breadth ratio x.

VII DISCUSSION AND CONCLUSIONS

The DiMarzio–Alben lattice model, even as modified in Section II, has been shown to display a number of very serious deficiencies, whether treated in the Bragg–Williams or the quasi-chemical approximation. For $x \geq 5$, $P = 1$ atm and reasonable values of segmental attractive energies, the system goes directly from an ordered liquid to an isotropic gas. Even when the pressure and attractive energies are adjusted to eliminate this difficulty and produce reasonable transition temperatures, the model predicts (1) an almost perfectly ordered nematic mesophase all the way to the N → I transition (2) relative density discontinuities at the N → I transition of the order of 50%; (3) a strong dependence of the N → I transition densities on the molecular length-to-breadth ratio x (4) rapidly increasing N → I transition temperatures coupled with little change in ΔS_{trans} as the molecular "tails" are lengthened—all in sharp contrast to experimentally observed behavior. Of these defects, only the very high degrees of order are unique to the lattice model as opposed to continuum models, where all molecular positions and orientations are allowed. (The near-perfect orientational order is not surprising given the restriction to three mutually orthogonal orientations which does not permit the sort of small angle deviations from the preferred direction which account for the orientational disorder in real nematic mesophases.)

The exaggerated length dependence of the transition densities and the sharp increases in $T_{N \to I}$ as the rods become longer seem to be standard behavior for model systems with hard, inflexible, rodlike molecular cores, at least in "molecular field" treatments where short-range orientational and translational order are neglected. Furthermore, at least in the scaled particle approach,[16] when a van der Waal's attractive term $-NWv_0p$, with W of order 10^4 K and $P = 1$ atm, is added to the Helmholtz free energy expression for a fluid of hard rods (all orientations permitted), the relative density discontinuity $(\rho_{\text{nem}} - \rho_{\text{iso}})/\rho_{\text{nem}}$ increases rapidly with increasing length-to-breadth ratio of the rods until for x of order 10, the system vaporizes directly from the nematic phase. Although a stable isotropic liquid can be obtained by increasing the pressure by roughly an order of magnitude, the model then predicts relative N → I density discontinuities of the order of 50% for longer rods.[35] This behavior, like that of the lattice model, may well result to a large extent from treating the hard core repulsions in the molecular field approximation. As Alben[21] has convincingly argued, the complete neglect of short-range order leads to an underestimation of the number of allowed N-body configurations, and hence of the configurational entropy, that becomes more severe as the density increases or the rods are lengthened or the system becomes more disordered orientationally. The resulting entropic "discrimination" against the isotropic phase increases with increasing x and is enhanced by the addition of a density dependent intermolecular attractive energy, since at a particular temperature and pressure the system is more dense when nematic than when isotropic. Of course, the precise extent to which the model predictions are artifacts of the molecular field approximation cannot be determined since there are no exact or computer simulation results available concerning the order–disorder transition in a three-dimensional system of hard rods. Such results would obviously be extremely useful. Because of its relative simplicity compared to continuum systems, a system of hard rods on a well-defined lattice might be a promising candidate for consideration via the Monte Carlo or molecular dynamics technique.

As a consequence of the difficulties just described, molecular field treatments of long inflexible rodlike molecules with hard cores and superimposed intermolecular attractions (using a lattice or a continuum model) would appear to be of little use for investigating the way in which various molecular factors determine the relative stabilities of the nematic and isotropic phases in pure substances. Fortunately, many common thermotropic liquid crystals are not, in fact, inflexible, but are more accurately represented by model particles with inflexible central portions and semi-flexible end chains. It may be possible to treat a system of such particles profitably in the molecular field approximation, provided the rigid central portions are not too long.

Obviously a theoretical approach incorporating short-range order in some reasonably realistic manner would be extremely desirable.

Despite the inadequacies of the DiMarzio–Alben approach for one-component nematogenic systems it appears that the lattice model may well prove useful for investigating solute induced nematic → isotropic transitions in solutions with nonmesomorphic solutes and nematic solvents. Recently, Peterson, Martire, and Cotter[36] and Ågren and Martire[37] considered lattice systems of hard rods of two different lengths and of hard rods and cubes, respectively, and obtained results in surprisingly good qualitative agreement with experimental data.[38] In order to determine whether improved results can be obtained by adding segmental attractive interactions, or whether "pathological" behavior of the sort encountered in the one-component case will ensue, a very simple "test case" has been considered; namely, mixtures of hard rods of two different length-to-breadth ratios on a simple cubic lattice, with segmental attractive energies w_{ii}, w_{ij}, and w_{jj}, where i and j indicate a segment of a solvent and a solute rod, respectively. The partition function and various thermodynamic expressions for this simple model are derived in the Appendix and typical numerical results are presented in Figures 9 and 10 for a system with $x_i = 5$, $x_j = 2$, $w_{ii}/k = -100$ K,

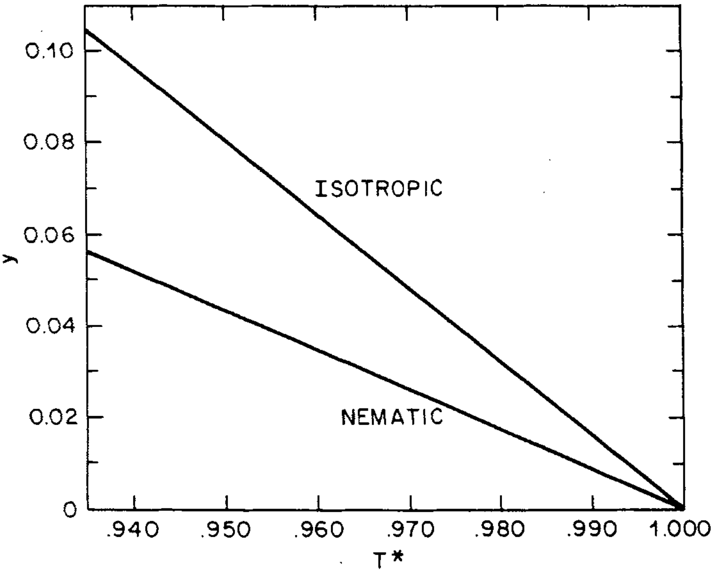

FIGURE 9 Solute mole fractions in the coexisting phases in the two-phase region as a function of the reduced temperature T^*.

$$\frac{w_{ii}}{k} = -150\text{ K}, \quad \frac{w_{jj}}{k} = -75\text{ K}, \quad w_{ij} = -\sqrt{w_{ii}w_{jj}}.$$

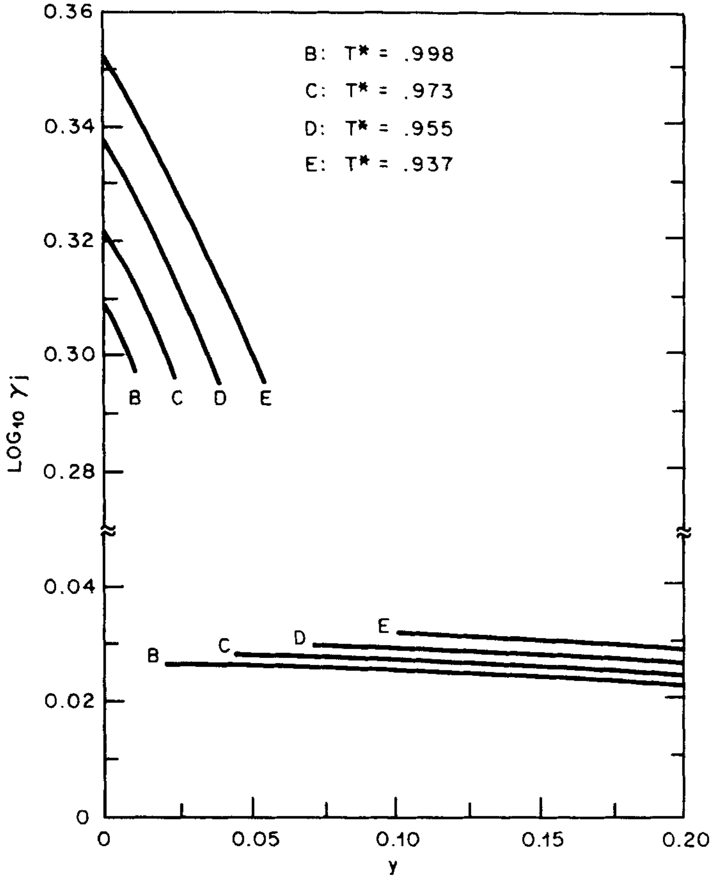

FIGURE 10 Common logarithm of the solute activity coefficient, $\log_{10}\gamma_j$, as a function of solute mole fraction y at four reduced temperatures.

$$\frac{w_{ii}}{k} = -150\text{ K},\quad \frac{w_{jj}}{k} = -75\text{ K},\quad w_{ij} = -\sqrt{w_{ii}w_{jj}}.$$

$w_{jj}/k = -50$ K, $w_{ij} = \sqrt{w_{ii}w_{jj}}$. In Figure 9, the solute mole fractions in the coexisting phases in the two-phase region are plotted versus the reduced temperature $T^* = T/T^0_{N\to I}$ ($T^0_{N\to I}$ is the N → I transition temperature for the pure solvent), while in Figure 10, the logarithm of the solute activity coefficient $\log_{10}\gamma_j$ is plotted versus solute mole fraction at several reduced temperatures. By comparing these figures with Figures 3–6 of Reference 38 (the same four values of T^* were used in Figure 10 as in Figures 3, 4, and 5 of Peterson and Martire), it can be seen that the model predictions are in quite respectable qualitative agreement with experiment. In fact, the agreement is better than that obtained with the hard rod model of Peterson, Martire, and Cotter[36] in at least two respects:

1) The values of $\log_{10} \gamma_j$ obtained are considerably more positive, and thus closer to the experimental data, than those predicted by the hard rod model.

2) For appropriate choices of the segmental energies (such as that of Figure 10), $\log_{10} \gamma_j$ slowly decreases with increasing solute mole fraction in the isotropic phase, whereas a small increase is predicted by the hard model.

The quite decent results obtained with this simple van der Waals model are quite encouraging. As noted by Peterson, Martire and Cotter, one is reminded of a similar situation in the theory of nonelectrolytes, where lattice models yield poor results for pure liquids but give a qualitatively decent account of the excess mixing properties of solutions.[39] The treatment of Section II can be extended readily to mixtures of rods or of rods and cubes, and it would seem worthwhile to do so.

Finally, as was noted in Section V, the reasonable account of certain aspects of the smectic A → nematic transition provided by the lattice model, despite the very crude treatment of the smectic mesophase, encourages one to hope that more sophisticated lattice models[40] and/or cell models might prove useful in determining the molecular factors governing the stabilities of smectic mesophases, both the more common smectics: A, B, and C, and the more "exotic" mesophases: D, E, F, G, H. Cell models appear particularly promising since the molecules are allowed to move about in the average cage created by their neighbors and can be permitted small angle rotations away from the preferred direction as well, thus enabling one to treat translational and orientational ordering in a somewhat more realistic manner. As a first step in this direction, a simple cell model has recently been used, with considerable success, to investigate the smectic A → nematic transition.[41]

References

1. W. Maier and A. Saupe, *Z. Naturforsch.*, **14a**, 882 (1959); **15a**, 287 (1960).
2. B. Deloche, B. Cabane, and D. Jerome, *Mol. Cryst., Liquid Cryst.*, **15**, 197 (1971).
3. J. R. McColl and C. S. Shih, *Phys. Rev. Letters*, **29**, 85 (1972).
4. R. L. Humphries, P. G. James, and G. R. Luckhurst, *Faraday Soc. Transactions* II, **68**, 1031 (1972).
5. S. Chandrasekhar and N. V. Madhusudana, *Acta Cryst.*, **A27**, 303 (1971).
6. W. L. McMillan, *Phys. Rev. A*, **4**, 1238 (1971).
7. F. T. Lee, H. T. Tan, Y. M. Shih, and C. Woo, *Phys. Rev. Letters*, **31**, 1117 (1973).
8. K. Miyakawa, N. Hijikuro, and H. Mori, *J. Phys. Soc. Japan*, **36**, 944 (1974).
9. R. J. Meyer and W. L. McMillan, *Phys. Rev. A*, **9**, 899 (1974).
10. S. Marčelja, *J. Chem. Phys.*, **60**, 3599 (1974).

11. P. J. Flory, *Statistical Mechanics of Chain Molecules*. (Interscience, New York, 1969), Chapter III.
12. R. Zwanzig, *J. Chem. Phys.*, **39**, 1714 (1963).
13. L. K. Runnels and C. Colvin, *J. Chem. Phys.*, **53**, 4219 (1970).
14. M. A. Cotter and D. E. Martire, *J. Chem. Phys.*, **53**, 4500 (1970).
15. G. Lasher, *J. Chem. Phys.*, **53**, 4141 (1970).
16. M. A. Cotter, *Phys. Rev. A*, **10**, 625 (1974).
17. K. M. Timling, *J. Chem. Phys.*, **61**, 465 (1974).
18. P. J. Flory, *Proc. Roy. Soc.* (London) **A234**, 73 (1956).
19. E. A. DiMarzio, *J. Chem. Phys.*, **35**, 658 (1961).
20. M. A. Cotter and D. E. Martire, *Mol. Cryst., Liquid Cryst.*, **7**, 295 (1969).
21. R. Alben, *Mol. Cryst., Liquid Cryst.*, **13**, 193 (1971).
22. A. Wulf and A. G. DeRocco, *J. Chem. Phys.*, **55**, 12 (1971).
23. G. Ågren and D. E. Martire, *J. Chem. Phys.*, **61**, 3959 (1974).
24. P. J. Flory, *J. Chem. Phys.*, **10**, 51 (1942).
25. When determining the v_{n+1}'s, one assumes that all the rods are distinguishable, then accounts for the indistinguishability of rods pointing in the same direction by dividing by $\prod_{i=1}^{3} N_i!$.
26. DiMarzio[19] evaluated the product $\prod_{\nu=0}^{N-1} v_{n+1}^{(k)}$ by adding first the N_1 rods in orientation 1, then the N_2 rods in orientation 2, then the N_3 rods in orientation 3. It can be shown, however, that the result does not depend on the order in which the rods are added.
27. T. L. Hill, *Statistical Mechanics* (McGraw-Hill, New York, 1956), Section 46.
28. P. J. Flory, *Principles of Polymer Chemistry* (Cornell University Press, Ithaca, New York, 1953) Chapter XII.
29. R. H. Fowler and E. A. Guggenheim, *Proc. Roy. Soc.* (London) **A174**, 189 (1940).
30. The very large density discontinuities at the N → I transition can be decreased somewhat by increasing the pressure on the system. The "price" one pays, however, is that T_{trans} rises considerably more rapidly with increasing length-to-breadth ratio x.
31. The order parameter η is most commonly measured by means of proton magnetic resonance, since uniformly oriented nematic samples can be produced by modest magnetic fields and the direct proton–proton couplings obtained are proportional to η. Saupe (A. Saupe, Angew. Chem. Intern. Ed. (English), 7, 97 (1968)) has summarized and discussed experimentally determined order parameters for common nematic liquids.
32. G. W. Gray, *Molecular Structure and the Properties of Liquid Crystals*. (Academic Press, New York, 1962), Chapter VIII.
33. Z. Luz and S. Meiboom, *J. Chem. Phys.*, **59**, 275 (1973); Z. Luz, R. C. Hewitt, and S. Meiboom, *J. Chem. Phys.*, **61**, 1758 (1974).
34. In the quasi-chemical as well as the Bragg–Williams approximation, the system boils from an ordered state (the nematic state when $w_{cc} = w_{tt}$) when atmospheric pressure and reasonable segmental attractive energies are used.
35. M. A. Cotter (unpublished). The same qualitative results are also obtained when an anisotropic free energy term $-W_a(v_0\rho)\eta^2/kT$ is added to the isotropic Van der Waals term, both when W_a and W_i are assumed to be independent of x and when they are taken to be proportional to x.
36. H. T. Peterson, D. E. Martire, and M. A. Cotter, *J. Chem. Phys.*, **61**, 3547 (1974).
37. G. Ågren and D. E. Martire, *J. Phys.*, **36**, Cl-141 (1975).
38. H. T. Peterson and D. E. Martire, *Mol. Cryst., Liquid Cryst.*, **25**, 89 (1974).
39. I. Prigogine (with the collaboration of V. Mathot and A. Bellemans), *The Molecular Theory of Solutions* (North Holland, Amsterdam, 1957).
40. In this vein, Miyakawa, Hijikuro, and Mori[8] studied a model system of rods of length-to-breadth ratio two (with anisotropic intermolecular attractions and repulsions) on a simple cubic lattice and observed four different phases corresponding to the gas, isotropic liquid, nematic and smectic phases. Because of their use of interleaved sublattices to define a smectic translational order parameter, however, their approach would be quite difficult to extend to longer rods.
41. G. C. Lin, Doctoral Dissertation, Georgetown University, 1975.

Appendix. The Simple Two-Component Mixture

The model system consists of a simple cubic lattice of M sites containing N_i hard inflexible solvent rods of length to breadth ratio x_i and N_j hard inflexible solute rods of length-to-breadth ratio x_j, with segmental attractive energies w_{ii}, w_{ij}, and w_{jj}, corresponding to solvent–solvent, solvent–solute, and solute–solute interactions respectively. Each rod of type v ($v = i$ or j) must occupy x_v adjacent lattice sites and can point in only three mutually perpendicular directions: 1, 2, and 3. In the thermodynamic limit, the Bragg–Williams configurational partition function can be written

$$Q_c = \Omega(M, N_{i1}^*, N_{i2}^*, N_{i3}^*, N_{j1}^*, N_{j2}^*, N_{j3}^*)\exp\left(-\frac{\bar{N}_{ii}w_{ii} + \bar{N}_{ij}w_{ij} + \bar{N}_{jj}w_{jj}}{kT}\right) \tag{A1}$$

where Ω is the number of ways to arrange N_{i1}^* solvent rods in orientation 1, N_{i2}^* solvent rods in orientation 2, ..., N_{j3}^* solute rods in orientation 3 on the lattice; $\bar{N}_{ii}$, $\bar{N}_{ij}$, and $\bar{N}_{jj}$ are the average number of pairs of nearest neighbor segments of the specified types (weighting all allowed configurations equally); and the asterisks denote that distribution which maximizes Q_c. Using the DiMarzio–Alben counting scheme, Peterson, Martire, and Cotter[36] derived an (approximate) expression for Ω, namely

$$\begin{aligned}\frac{1}{N}\ln\Omega = \frac{1}{\zeta}\{&2[1 - (x_i - 1)s\zeta_i - (x_j - 1)t\zeta_j]\ln[1 - (x_i - 1)s\zeta_i - (x_j - 1)t\zeta_j]\\ &+ [1 - (x_i - 1)(1 - 2s)\zeta_i - (x_j - 1)(1 - 2t)\zeta_j]\\ &\cdot\ln[1 - (x_i - 1)(1 - 2s)\zeta_i - (x_j - 1)(1 - 2t)\zeta_j]\\ &- 2s\zeta_i\ln s - (1 - 2)\zeta_i\ln(1 - 2s)\\ &- \zeta_i\ln\zeta_i - 2t\zeta_j\ln t - (1 - 2t)\zeta_j\ln(1 - 2t) - \zeta_j\ln\zeta_j\\ &-(1 - x_i\zeta_i - x_j\zeta_j)\ln(1 - x_i\zeta_i - x_j\zeta_j)\end{aligned}$$

where

$$\zeta_i = \frac{N_i}{M}, \quad \zeta_j = \frac{N_j}{M}, \quad \zeta = \zeta_i + \zeta_j, \quad s = \frac{N_{i2}^*}{N_i} = \frac{N_{i3}^*}{N_i}, \quad t = \frac{N_{j2}^*}{N_j} = \frac{N_{j3}^*}{N_j},$$

and it is assumed that the orientational distributions for both solute and solvent are axially symmetric about direction 1, the preferred direction.

$\bar{N}_{ii}$, $\bar{N}_{ij}$, and $\bar{N}_{jj}$ can also be determined using the same counting technique. For example,

$$2\bar{N}_{ii} = \sum_k N_{ii}^{(k)}$$

$$= \sum_k \frac{\{2N_{ik}^*[N_{ik}^* + x_i \sum_{l\neq k} N_{il}^*] + 2x_i \sum_{l\neq k} N_{il}^*[N_{ik}^* + x_i \sum_{l\neq k} N_{il}^*]\}}{M - (x_i - 1)N^*{}_{ik} - (x_j - 1)N_{jk}^*} \tag{A3}$$

$$\frac{\bar{N}_{ii}}{M} = \frac{\zeta_i^2[1 + 2(x_i - 1)s]^2}{1 - (x_i - 1)(1 - 2s)\zeta_i - (x_j - 1)(1 - 2t)\zeta_j} + \frac{2\zeta_i^2[x_i - (x_i - 1)s]^2}{1 - (x_i - 1)s\zeta_i - (x_j - 1)t\zeta_j}, \tag{A4}$$

where $N_{ii}^{(k)}$ is the average number of pairs of nearest neighbor segments in which a solvent rod is adjacent in direction k to another solvent rod. Similarly, it is easily seen that

$$\frac{\bar{N}_{jj}}{M} = \frac{\zeta_j^2[1 + 2(x_j - 1)t]^2}{1 - (x_i - 1)(1 - 2s)\zeta_i - (x_j - 1(1 - 2t)\zeta_j} + \frac{2\zeta_j^2[x_j - (x_j - 1)t]^2}{1 - (x_i - 1)s\zeta_i - (x_j - 1)t\zeta_j} \tag{A5}$$

$$\frac{\bar{N}_{ij}}{M} = \frac{2\zeta_i\zeta_j[1 + 2(x_i - 1)s][1 + 2(x_j - 1)t]}{1 - (x_i - 1)(1 - 2s)\zeta_i - (x_j - 1)(1 - 2t)\zeta_j} + \frac{4\zeta_i\zeta_j[x_i - (x_i - 1)s][x_j - (x_j - 1)t]}{1 - (x_i - 1)s\zeta_i - (x_j - 1)t\zeta_j} \tag{A6}$$

The configurational contribution to all the thermodynamic functions of the system can be obtained from Q_c. In particular

$$\Phi = \frac{Pv_0}{kT} = \ln R_1 + 2\ln R_2 - \ln R_3 + \frac{\zeta^2}{kT}\left\{\frac{R_8}{R_1^2} + \frac{2R_9}{R_1^2}\right\} \tag{A7}$$

$$\begin{aligned}\frac{\mu_i}{kT} = {} & (x_i - 1)[(1 - 2s)\ln R_1 + 2s\ln R_2] - x_i \ln R_3 + \ln[(1 - y)\zeta] \\ & + (1 - 2s)\ln(1 - 2s) + 2s\ln s \\ & + \frac{2\zeta}{kT}\left\{\frac{[1 + 2(x_i - 1)s]R_4}{R_1} + \frac{[x_i - (x_i - 1)s]R_5}{R_2}\right\} \\ & + \frac{\zeta^2}{kT}\left\{\frac{(x_i - 1)(1 - 2s)R_8}{R_1^2} + \frac{2(x_i - 1)sR_9}{R_2^2}\right\}\end{aligned} \tag{A8}$$

$$\begin{aligned} \frac{\mu_j}{kT} &= (x_j - 1)[(1 - 2t)\ln R_1 + 2t \ln R_2] - x_j \ln R_3 + \ln(y\zeta) \\ &\quad + \frac{2\zeta}{kT}\left\{\frac{[1 + 2(x_j - 1)t]R_6}{R_1} + \frac{[x_j - (x_j - 1)t]R_7}{R_2}\right\} \\ &\quad + \frac{\zeta^2}{kT}\left\{\frac{(x_j - 1)(1 - 2t)R_8}{R_1^2} + \frac{2(x_j - 1)tR_9}{R_2^2}\right\} \end{aligned} \tag{A9}$$

$$\ln \gamma_j = \frac{\mu_j}{kT} - \frac{\mu_j^*}{kT} - \ln y, \tag{A10}$$

where y is the solute mole fraction, μ_j^* the configurational chemical potential of pure solute at the same temperature and pressure as the solution, γ_j the solute activity coefficient, and

$$\begin{aligned} R_1 &= 1 - (x_i - 1)(1 - 2s)(1 - y)\zeta - (x_j - 1)(1 - 2t)y\zeta \\ R_2 &= 1 - (x_i - 1)s(1 - y)\zeta - (x_j - 1)ty\zeta \\ R_3 &= 1 - x_i(1 - y)\zeta - x_j y\zeta \\ R_4 &= (1 - y)[1 + 2(x_i - 1)s]w_{ii} + y[1 + 2(x_j - 1)t]w_{ij} \\ R_5 &= (1 - y)[x_i - (x_i - 1)s]w_{ii} + y[x_j - (x_j - 1)t]w_{ij} \\ R_6 &= y[1 + 2(x_j - 1)t]w_{jj} + (1 - y)[1 + 2(x_i - 1)s]w_{ij} \\ R_7 &= y[x_j - (x_j - 1)t]w_{jj} + (1 - y)[x_i - (x_i - 1)s]w_{ij} \\ R_8 &= (1 - y)[1 + 2(x_i - 1)s]R_4 + y[1 + 2(x_j - 1)t]R_6 \\ R_9 &= (1 - y)[x_i - (x_i - 1)s]R_5 + y[x_j - (x_j - 1)t]R_7. \end{aligned} \tag{A11}$$

s, t, and ζ can be determined at a particular T, P, and y by solving the set of simultaneous equations

$$\Phi(\zeta, s, t) = \frac{Pv_0}{kT} \tag{A12}$$

$$0 = \ln\left(\frac{R_2}{R_1}\right) + (x_i - 1)^{-1} \ln\left(\frac{s}{1 - 2s}\right) + 2\zeta\frac{R_4}{R_1} - \frac{\zeta^2 R_6}{R_1} - \frac{\zeta R_5}{R_2} + \frac{\zeta^2 R_9}{R_2^2} \tag{A13}$$

$$\begin{aligned} 0 &= \ln\left(\frac{R_2}{R_1}\right) + (x_j - 1)^{-1} \ln\left(\frac{t}{1 - 2t}\right) + 2\zeta\left(\frac{R_6}{R_1}\right) \\ &\quad - \zeta^2\left(\frac{R_8}{R_1^2}\right) - 2\zeta\left(\frac{R_7}{R_2^2}\right) + \zeta^2\left(\frac{R_9}{R_2^2}\right) \end{aligned} \tag{A14}$$

where $\Phi(\zeta, s, t)$ is given by (A7) and (A13) and (A14) were derived by maximizing $\ln Q_c$ (minimizing A) with respect to s and t, respectively. Finally, the two-phase region can be located at a particular T and P by simultaneously solving

$$\Phi(\zeta_{\mathrm{nem}} s, t) = \frac{Pv_0}{kT}, \tag{A15}$$

$$\Phi(\zeta_{\mathrm{iso}}, \tfrac{1}{3}, \tfrac{1}{3}) = \frac{Pv_0}{kT}, \tag{A16}$$

$$\frac{\mu_i}{kT}(\zeta_{\mathrm{nem}}, s, t) = \frac{\mu_i}{kT}(\zeta_{\mathrm{iso}}, \tfrac{1}{3}, \tfrac{1}{3}), \tag{A17}$$

$$\frac{\mu_j}{kT}(\zeta_{\mathrm{nem}}, s, t) = \frac{\mu_j}{kT}(\zeta_{\mathrm{iso}}, \tfrac{1}{3}, \tfrac{1}{3}), \tag{A18}$$

together with (A13) and (A14).